

EXPLOSIVE NUCLEOSYNTHESIS CLOSE TO THE DRIP LINES *

F.-K. THIELEMANN^{a,e}, C. FREIBURGHaus^a, T. RAUSCHER^a,
F. REMBGES^a, S. ROSSWOG^a, B. PFEIFFER^b K.-L. KRATZ^b,
H. SCHATZ^c AND M.C. WIESCHER^d

^aDepartement für Physik und Astronomie, Universität Basel
Klingelbergstr. 82, CH-4056 Basel, Switzerland

^bInstitut für Kernchemie, Universität Mainz
Fritz-Strassmann-Weg 2, D-55099 Mainz, Germany

^cGesellschaft fuer Schwerionenforschung mbH, D-64291 Darmstadt, Germany

^dDepartment of Physics, University of Notre Dame
Notre Dame, IN 46556, USA

^ePhysics Division, Oak Ridge National Laboratory
Oak Ridge, TN 37831-6371, USA

(Received October 9, 1998)

We give an overview of explosive burning and the role which neutron and/or proton separation energies play. We focus then on the rapid neutron capture process (r-process) which encounters unstable nuclei with neutron separation energies in the range 1–4 MeV, and the rapid proton capture process (rp-process), operating close to the proton drip-line. The site of the rp-process is related to hydrogen accreting neutron stars in binary stellar systems. Explosive H-burning produces nuclei as heavy as $A=100$, powering events observable as X-ray bursts. The r-process abundances witness nuclear structure far from beta-stability as well as the conditions in the appropriate astrophysical environment. But there is a remaining lack in the full understanding of its astrophysical origin, ranging from the high entropy neutrino wind, blown from hot neutron star surfaces after a supernova explosion, to low entropy “cold decompression” of neutron star matter ejected in mergers of binary neutron star systems.

PACS numbers: 21.10.Dr, 23.40.-s, 97.10.Vc, 98.35.Bd

* Presented at the MESON '98 and Conference on the Structure of Meson, Baryon and Nuclei, Cracow, Poland, May 26–June 2, 1998.

1. Introduction

Hydrostatic burning stages in stellar evolution, like H, He, C, and Ne-burning with temperatures being essentially confined to $T < 10^9$ K, are dominated by individual nuclear reactions and the precision of their cross sections. The same is true for explosive events which never surpass critical temperatures, like *e.g.* explosive H-burning in novae with temperatures $T < 3 \times 10^8$ K or also some explosive burning stages in supernovae. For other explosive events individual reactions matter strongly during their ignition stages, *e.g.* in explosive H-burning in X-ray bursts break-out reactions from the hot CNO-cycle (bridging the gap between CNO nuclei and Ne) and other hot CNO-type cycles up to Ti are important. This applies also to central C-ignition in white dwarf progenitors of type Ia supernovae.

However, a whole variety of burning processes responsible for the abundances of intermediate and heavy nuclei, like *e.g.* hydrostatic Si and explosive O and Si-burning, are leading to partial (quasi) or full equilibria of reactions (QSE or NSE). These are described by the chemical potentials of nuclei which form a Boltzmann gas. The abundance ratios are (besides thermodynamic environment properties) determined by mass differences. Therefore, mass uncertainties matter, but uncertainties in cross sections do not enter abundance determinations. Non-equilibrium regions are identified by small cross sections either due to small Q -values for reactions out of the magic numbers or due to small level or resonance densities for light nuclei. For sufficiently high temperatures all QSE groups merge to a full NSE.

The chemical equilibrium for neutron or proton captures leads to abundance maxima at specific neutron or proton separation energies

$$\frac{Y(A_c)}{Y(A_t)} = n_p \frac{G(A_c)}{g_p G(A_t)} \left[\frac{A_c}{A_p A_t} \right]^{3/2} \left[\frac{2\pi\hbar^2}{m_u kT} \right]^{3/2} \exp(S_p(A_c)/kT), \quad (1)$$

$$\frac{S_p(A_c)}{kT} = 24 \ln \left[\left(\frac{A_t A_p}{A_c} \right)^{3/2} \left(\frac{G(A_t) g_p}{2G(A_c)} \right)^{3/2} \left(\frac{T}{10^9 \text{K}} \right)^{3/2} \frac{N_A}{n_p / \text{cm}^3} \right]. \quad (2)$$

The equations are valid for neutron, proton (and/or alpha) captures, as indicated by the p (projectile) subscript t stands for target and c for the compound nucleus. The Y 's are abundances related to number densities n via $n = \rho N_A Y$. At the maximum in an isotopic or isotonic line we have $S_{p=n \text{ or } p} \approx 24$ kT, if the partition functions G are neglected (order unity). This is slightly modified by logarithmic dependences on density and temperature. When an equilibrium with neutrons and protons exists, the abundance maximum is found in the nuclear chart at the intersection of the relevant neutron and proton separation energies. The free neutron and

proton densities reflect the total neutron/proton ratio in matter, which is determined by slow, weak interactions not in equilibrium by changing Y_e , the total proton/nucleon ratio $Y_e = \langle Z/A \rangle$.

The understanding that explosive burning stages are governed by QSE or even NSE is growing [13, 14, 57, 59]. This has been shown recently in calculations of type II supernova nucleosynthesis [17, 52] with two libraries of nuclear reaction rates [36, 50, 53, 60]. Of the nuclei produced in explosive O and Si-burning, only abundance differences were noticed in the transition region between the Si and Fe groups. Different types of QSE-groups can emerge in explosive burning. The high temperature phase of the rp-process in X-ray bursts witnesses isotonic lines in $(p, \gamma) - (\gamma, p)$ equilibrium, because neutrons are not available in hydrogen-rich layers [38, 41]. Another application is the r-process, here the QSE-groups are isotopic lines in $(n, \gamma) - (\gamma, n)$ equilibrium. The connecting weak interactions for both processes are β^+ or β^- -decays. During the final reeze-out from equilibria when temperatures decline below equilibrium conditions, reaction rates count again.

In general it should be pointed out that equilibria simplify the understanding of explosive nucleosynthesis processes and individual cross sections play a much less important role than reaction Q-values. However, the rp and r-process explore exotic nuclei close to the neutron or proton drip-lines where also masses are not well known. Therefore, the focus lies on nuclear masses and beta-decay properties.

2. The rp-process and X-ray bursts

The major astrophysical events which involve explosive H-burning are novae and type I X-ray bursts. Both are related to binary stellar systems with hydrogen accretion from a binary companion onto a compact object, and the explosive ignition of the accreted H-layer. High densities cause the pressure to be dominated by the degenerate electron gas, preventing a stable and controlled burning. In the case of novae the compact object is a white dwarf, in the case of X-ray bursts it is a neutron star. Explosive H-burning in novae has been discussed in many recent articles [4, 12, 20, 45]. Its processing is limited due to maximum temperatures of $\sim 3 \times 10^8$ K. Only in X-ray bursts temperatures larger than 4×10^8 K are possible.

In type I X-ray bursts [25, 46, 47] hydrogen (and helium) burn explosively in a thermonuclear runaway. In essentially all nuclei below Ca, the proton capture reaction on nucleus $(Z_{\text{even}}-1, N=Z_{\text{even}})$ produces the compound nucleus above the alpha-particle threshold and permits a (p, α) reaction. This is typically not the case for $(Z_{\text{even}}-1, N=Z_{\text{even}}-1)$ due to the smaller proton separation energy, which leads to hot CNO-type cycles above Ne. There is one exception, $Z_{\text{even}}=10$, where the reaction $^{18}\text{F}(p, \alpha)$ is possible, avoiding

^{19}F and a possible leak via $^{19}\text{F}(p, \gamma)$ into the NeNaMg-cycle. This has the effect that only alpha induced reactions like $^{15}\text{O}(\alpha, \gamma)$ can aid a break-out from the hot CNO-cycle to heavier nuclei beyond Ne.

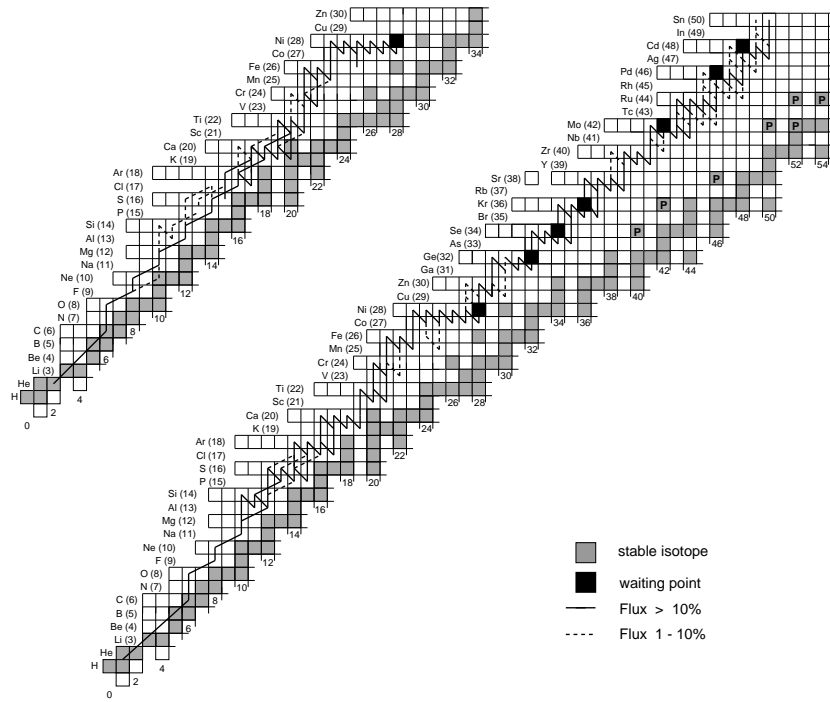


Fig. 1. rp and ap-process flow up to and beyond Ni. The reaction flows shown in the nuclear chart are integrated reaction fluxes from a time dependent network calculation [41,42], (a) during the initial burst and thermal runaway phase of about 10s, (b) after the onset of the cooling phase when the proton capture on ^{56}Ni is not blocked anymore by photodisintegrations (extending for about 200s). Waiting points above ^{56}Ni are represented by filled squares, stable nuclei by hatched squares, light p-process nuclei below $A=100$ are indicated by a *P*.

Once such temperatures are exceeded, also He is burned via the 3α -reaction and the αp -process (a sequence of (α, p) and (p, γ) reactions), which provides seed nuclei for hydrogen burning via the rp-process [38, 56]. Processing of the rp-process beyond ^{56}Ni is shown in Fig. 1 [41, 42]. Certain nuclei play the role of long waiting points in the reaction flux, where long beta-decay half-lives dominate the flow, either competing with slow (α, p) reactions or negligible (p, γ) reactions, because they are inhibited by inverse photodisintegrations for the given temperatures. Such nuclei were identified as ^{25}Si ($\tau_{1/2}=0.22\text{s}$), ^{29}S (0.187s), ^{34}Ar (0.844s), ^{38}Ca (0.439s) [51]. The

bottle neck at ^{56}Ni can only be bridged for minimum temperatures around 10^9K (in order to overcome the proton capture Coulomb barrier), maximum temperatures below $2 \times 10^9\text{K}$ (in order to avoid photodisintegrations), and high densities exceeding 10^6g cm^{-3} [37, 41]. If this bottle neck can be overcome, other waiting points like ^{64}Ge (64s), ^{68}Se (96s), ^{74}Kr (17s) seem to be hard to pass. However, partially temperature dependent half-lives (due to excited state population), or mostly 2p-capture reactions (introduced in [11] and applied in [41]) can help. Such hold-ups will introduce a time structure in energy generation, and the question is whether they might even show up in light curves of bursts.

Our results, with an updated and complete reaction network between Ni and Sn, are shown in shown in Fig. 1. If only a small percentage of the matter escapes the strong gravitational field of the neutron star, some proton-rich stable nuclei (for historical reasons called *p*-process nuclei) below $A=100$ could be explained in the solar system abundances.

3. The r-process

The question whether we understand fully all astrophysical sites leading to an r-process is not a settled one. It is usually assigned to type II supernovae (SNe II), the events accompanying the deaths of massive stars and formation of neutron stars (high entropy ejecta, [48, 62]). But the delayed emergence of r-process matter in galactic evolution indicates that these can probably only be SNe II with small progenitor star mergers or still other low entropy sites are not necessarily excluded [9, 24, 27]. Recent observations shed some doubts on the supernova origin. On average SNe II produce Fe to intermediate mass elements in ratios within a factor of 3 of solar [52]. If they would also be responsible for the r-process, the same limits should apply. But the observed bulk r-process/Fe ratios vary widely in low metallicity stars. In CS 22892–052 the r/Fe ratio is 30 times solar [43]!

The observations of stellar spectra are all consistent with the solar r-abundance pattern of elements and the relative abundances among heavy elements do apparently not show any time evolution [5, 43], at least for elements heavier than Ba. This suggests that all events produce the same relative r-process abundances, but a single astrophysical site will still have varying conditions in different ejected mass zones (*i.e.* a superposition of components). A component is defined by a combination of neutron number density, temperature (defining the neutron separation energy of an r-process path) and duration time, or more physically for an adiabatic expansion, entropy, Y_e , and an expansion timescale. The physical conditions must vary smoothly, as expected from a single astrophysical site.

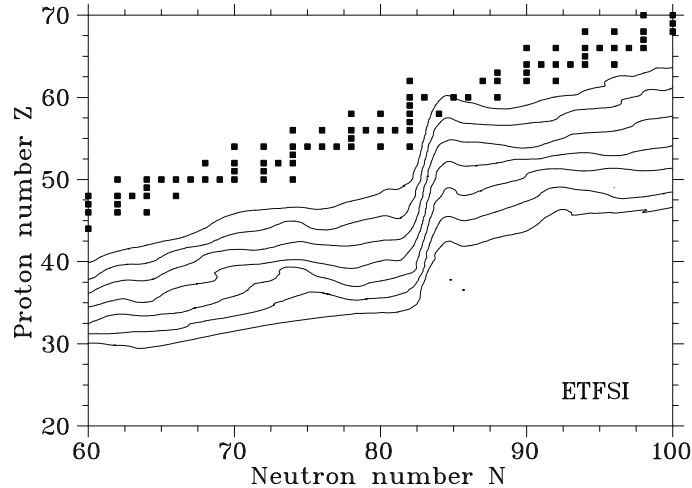


Fig. 2. Contour plots of constant neutron separation energies $S_n=1,2,3,4,5,6$, and 7 MeV in the $80 \leq A \leq 140$ mass region for the ETFSI mass model [1]. Note the saddle point behavior caused by the shell closure at $N = 82$, also existing when using the FRDM masses [30], which leads to a deep trough before the peak at $A = 130$ (see dashed line in Fig. 3).

The site-independent classical analysis of Kratz *et al.* [21, 22], based on n_n , T , and τ , led to the conclusion that the r-process experienced a fast drop from equilibrium (of the order of 0.05 s, at least for conditions producing the $A \simeq 80$ peak), in order not to wash out the odd-even staggering via slow freeze-out effects. A continuous superposition of components with neutron separation energies in the range 4 - 2 MeV (see Eq. (2), related to n_n and T) on timescales of 1 - 2.5 s, provided a good overall fit. The beta-decay properties along contour lines of constant S_n towards heavy nuclei [51] (see Fig. 2 for the region around the $N=82$ shell closure) are responsible for the resulting abundance pattern. These are predominantly nuclei not accessible in laboratory experiments to date. Exceptions exist in the $A = 80$ and 130 peaks [21, 22] and continuous efforts are underway to extend experimental information in these regions of the closed shells $N=50$ and 82 with radioactive ion beam facilities. Such classical r-process studies were extended to deduce necessary requirements for nuclear properties like masses, half-lives, and deformation [3, 34, 51]. One of the major conclusions was the quest for shell quenching far from stability in order to avoid abundance deficiencies, as seen in Fig. 3. Similar conclusions were drawn from more realistic, entropy-based calculations [10] and are not changed due to neutrino interactions with matter [28, 35]. Such quenching is also observed experimentally and predicted theoretically [8, 18, 23, 32, 44, 63].

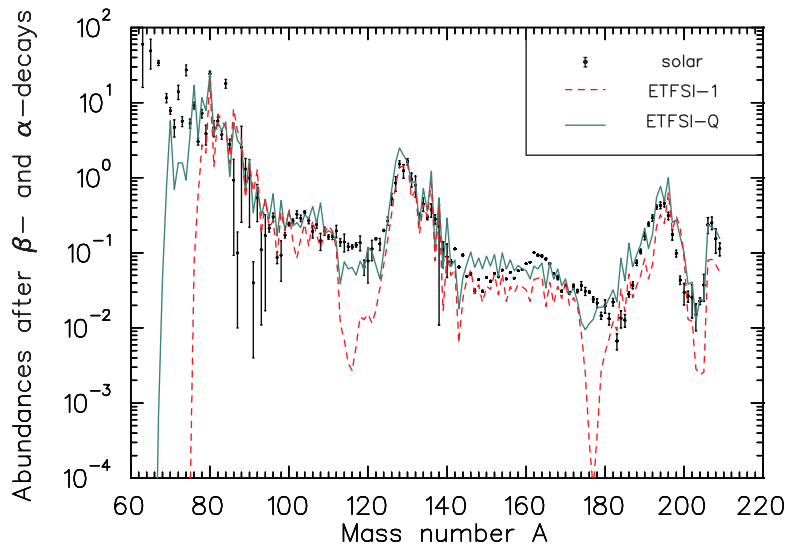


Fig. 3. Fits to solar r-process abundances, obtained with a smooth superposition of 17 equidistant $S_n(n_n, T)$ components from 1 to 4 MeV. The dashed line presents the results for ETFSI masses [1] with half-lives $\tau_{1/2}$ and beta-delayed neutron emission P_n values from QRPA calculations [29]. For the solid line the ETFSI-Q mass model [33] was applied, which introduced a phenomenological quenching of shell effects. The quenching of the $N = 82$ shell gap leads to a filling of the abundance troughs. These results [34] are also the first ones which show a good fit to the r-process Pb and Bi contributions after following the decay chains of unstable heavier nuclei.

4. Stellar r-process sites

An r-process requires 10 to 150 neutrons per seed nucleus (in the Fe-peak or somewhat beyond) have to be available to form all heavier r-process nuclei by neutron capture. For a composition of Fe-group nuclei and free neutrons that translates into a $Y_e = \langle Z/A \rangle = 0.12-0.3$. Such a high neutron excess is only possible for high densities in neutron stars under beta equilibrium ($e^- + p \leftrightarrow n + \nu$, $\mu_e + \mu_p = \mu_n$), based on the high electron Fermi energies which are comparable to the neutron-proton mass difference [27].

Another option is a so-called extremely alpha-rich freeze-out in complete Si-burning with moderate $Y_e > 0.40$. After the freeze-out of charged particle reactions in matter which expands from high temperatures but relatively low densities, *e.g.* 90% of all matter can be locked into ${}^4\text{He}$ with $N=Z$, which leaves even for moderate Y_e 's a large neutron/seed ratio for the few existing heavier nuclei. This corresponds to a freeze-out from QSE with an extremely weak connection between the light and heavy QSE groups due to

low densities. The links across the particle-unstable $A = 5$ and 8 gaps is only possible via the three body reactions $\alpha\alpha\alpha$ and $\alpha\alpha n$ to ^{12}C and ^9Be , whose reaction rates show a quadratic density dependence. The entropy can be used as a measure of the ratio between the remaining He mass-fraction and heavy nuclei. Similarly, the ratio of neutrons to heavy nuclei (*i.e.* the neutron to seed ratio) is a function of entropy and permits for high entropies, with large remaining He and neutron abundances compared to small heavy seed abundances, neutron captures which proceed to form the heaviest r-process nuclei [15, 16, 48, 61, 62].

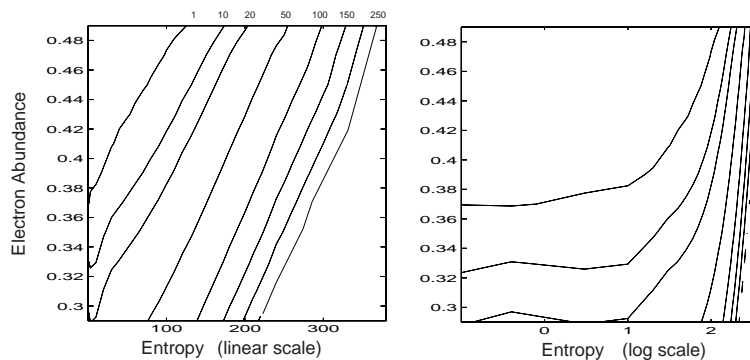


Fig. 4. Y_n/Y_{seed} contour plots as a function of initial entropy S and Y_e for an expansion time scale of 0.05s. The left part shows how, for moderate Y_e -values, an increasing neutron/seed ratio, indicated by contour lines labeled with the respective Y_n/Y_{seed} , can be attained with increasing entropy. The results scale with Y_e , measuring the global proton/nucleon ratio. The right part of the figure enhances on a logarithmic scale the low entropy behavior, where Y_n/Y_{seed} is only determined by the electron abundance Y_e . The contour lines are the same for both figures.

The behavior of these latter two environments, representing a normal and alpha-rich freeze-out, is summarized in Fig. 4. The available number of neutrons per heavy nucleus Y_n/Y_{seed} after charged particle freeze-out, when the large QSE-groups break up into isotopic lines, is shown as a function of entropy and initial Y_e . At low entropies the transition to a normal freeze-out occurs, indicated by the negligible entropy dependence. Recent r-process studies [16, 48, 62] have concentrated on the high entropy environment in the innermost ejecta of SNe II. Whether the required entropies can really be attained in supernova explosions has still to be verified.

An alternative site are neutron star mergers. Interest in a scenario where a binary system consisting of two neutron stars (ns-ns binary), loses energy and angular momentum through the emission of gravitational waves comes from various sides. Such systems are known to exist, five ns-ns binaries have been detected by now [54]. The measured orbital decay gave the first

evidence for the existence of gravitational radiation [49]. Further interest in the inspiral of a ns-ns binary arises from the fact that it is the prime candidate for a detection by the gravitational wave detector facilities that will go into operation in the very near future. A merger of two neutron stars may also lead to the ejection of neutron-rich material and may be a good site for the production of r-process elements. It is possible that such mergers account for all heavy r-process material in the Galaxy [9, 24]. The decompression of cold neutron star matter has been studied [24, 27]. However, a hydrodynamical calculation coupled with a complete r-process calculation has not been undertaken, yet.

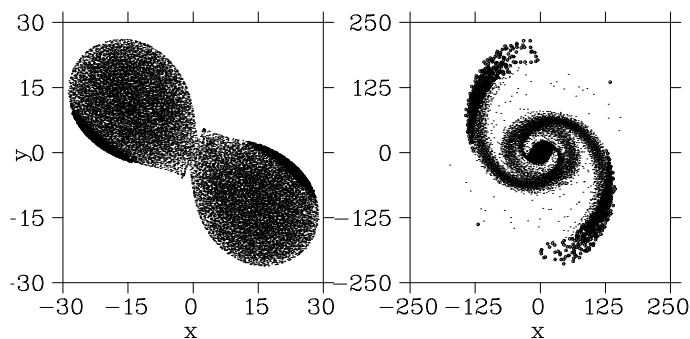


Fig. 5. Time evolution of a binary neutron star merger event at the moment of contact and 3 ms later. The SPH particles displayed in bold become unbound and escape (typically of the order $10^{-2}M_{\odot}$). [40]

The rate of neutron star mergers has been estimated to be of the order $10^{-6} - 10^{-5} \text{y}^{-1}$ per galaxy [9, 31], most recent estimates [55] tend towards the higher end of this range ($8 \cdot 10^{-6} \text{y}^{-1}$ per galaxy). Hydrodynamic simulations of neutron-star mergers are a formidable task. Beyond 3D hydrodynamics it should include general relativistic effects, employ a realistic equation of state, contain neutrino transport and neutrino cooling, and possible nuclear reactions [2, 7, 19, 26, 39]. In our study we used a 3D smooth particle hydrodynamics (SPH) code which does not use a spatial computational grid, but approximates “grid cells” by “particles” of the relevant mass. We [40] have performed extensive ns-ns merger calculations. Fig. 5 shows the time evolution of a merger event shortly before and 4 ms after merging of the two neutron stars. The particles displayed in bold become unbound and escape (typically of the order $10^{-2}M_{\odot}$). This is sufficient to reproduce the solar system r-process abundances, provided (which still needs to be shown) that this matter is converted into an r-process abundance pattern. SNe II still have to prove the correct environment conditions and given the galactic occurrence frequency, would need to eject $\sim 10^{-5} M_{\odot}$ per event.

This work was supported by the Swiss Nationalfonds (grant 20-47252.96 and 2000-053798.98), the German BMBF (grant 06Mz864) and DFG (grant Kr80615), the US NSF (grant PHY94-02761) and DOE (contracts DE-AC05-96OR22464 and DE-FG02-95-ER40934) and the Austrian Academy of the Sciences.

REFERENCES

- [1] Y. Aboussir, *et al.*, *At. Data Nucl. Data Tables* **61**, 127 (1995).
- [2] T.W. Baumgarte *et al.*, *Phys. Rev. Lett.* **79**, 1182 (1997).
- [3] B. Chen *et al.*, *Phys. Lett.* **B355**, 37 (1995).
- [4] A. Coc *et al.*, *J. Astrophys. Astron.* **299**, 479 (1995).
- [5] J.J. Cowan, A. McWilliam, C. Sneden, D.L. Burris, *Astrophys. J.* **480**, 246 (1997).
- [6] J.J. Cowan, F.-K. Thielemann, J.W. Truran, *Phys. Rep.* **208**, 267 (1991).
- [7] M.B. Davies, W. Benz, T. Piran, F.-K. Thielemann, *Astrophys. J.* **431**, 742 (1994).
- [8] J. Dobaczewski *et al.*, *Phys. Rev.* **C53**, 2809 (1996).
- [9] D. Eichler, M. Livio, T. Piran, D.N. Schramm, *Nature* **340**, 126 (1989).
- [10] C. Freiburghaus *et al.*, *Astrophys. J.*, in press 1998.
- [11] J. Görres, M. Wiescher, F.-K. Thielemann, *Phys. Rev.* **C51**, 392 (1995).
- [12] M. Hernanz, J. José, A. Coc, J. Isern, *Astrophys. J.* **465**, L27 (1996).
- [13] W.R. Hix, F.-K. Thielemann, *Astrophys. J.* **460**, 869 (1996).
- [14] W.R. Hix, F.-K. Thielemann, *Astrophys. J.*, in press 1998.
- [15] R.D. Hoffman *et al.*, *Astrophys. J.* **460**, 478 (1996).
- [16] R.D. Hoffman, S.E. Woosley, Y.Z. Qian, 1997, *Astrophys. J.* **482**, 951 (1997).
- [17] R.D. Hoffman, S.E. Woosley, T.A. Weaver, T. Rauscher, F.-K. Thielemann, submitted to *Astrophys. J.*, 1998.
- [18] R.W. Ibbotson *et al.*, *Phys. Rev. Lett.* **80**, 2081 (1998).
- [19] H.T. Janka, M. Ruffert, *Astron. Astrophys.* **307**, L33 (1996).
- [20] J. Jose, M. Hernanz, A. Coc, *Astrophys. J.* **479**, L55 (1997).
- [21] K.-L. Kratz *et al.*, *J. Phys. G* **14**, 331 (1988).
- [22] K.-L. Kratz, *et al.*, *Astrophys. J.* **402**, 216 (1993).
- [23] G.A. Lalazissis, D. Vretenar, P. Ring, *Phys. Rev.* **C57**, 2294 (1998).
- [24] J.M. Lattimer *et al.*, *Astrophys. J.* **213**, 225 (1977).
- [25] W.H.G. Lewin, J. van Paradijs, R.E. Taam, *Space Sci. Rev.* **62**, 223 (1993).
- [26] J.C. Lombardi, F.A. Rasio, *Phys. Rev.* **D56**, 3416 (1997).
- [27] B.S. Meyer, *Astrophys. J.* **343**, 254 (1989).
- [28] B.S. Meyer, G.C. McLaughlin, G.M. Fuller, *Phys. Rev.* **C**, in press, 1998.
- [29] P. Möller, J.R. Nix, K.-L. Kratz, *At. Data Nucl. Data Tables* **66**, 131 (1997).
- [30] P. Möller *et al.*, *At. Data Nucl. Data Tables* **59**, 185 (1995).

- [31] R. Narayan, B. Paczynski, T. Piran, *Astrophys. J.* **395**, L83 (1992).
- [32] N.A. Orr, 1991, *Phys. Lett.* **B258**, 29 (1991).
- [33] J.M. Pearson, R.C. Nayak, S. Goriely, *Phys. Lett.* **B387**, 455 (1996).
- [34] B. Pfeiffer, K.-L. Kratz, F.-K. Thielemann, *Z. Phys.* **A357**, 235 (1997).
- [35] Y.-Z. Qian, *et al.*, *Phys. Rev.* **C55**, 1532 (1996).
- [36] T. Rauscher, F.-K. Thielemann, K.-L. Kratz, *Phys. Rev.* **C56**, 1613 (1997).
- [37] E. Rehm, *et al.*, *Phys. Rev. Lett.* **80**, 676 (1998).
- [38] F. Rembges *et al.*, 1997, *Astrophys. J.* **484**, 412 (1997).
- [39] M. Ruffert, H.T. Janka, G. Schäfer, *Astron. Astrophys.* **319**, 122 (1997).
- [40] S. Rosswog, *et al.*, *Astron. Astrophys.*, in press, 1998.
- [41] H. Schatz, *et al.*, *Phys. Rep.* **294**, 167 (1998a).
- [42] H. Schatz, *et al.*, *AIP Conf. Proc.* **425**, 559 (1998b).
- [43] C. Sneden, *et al.*, *Astrophys. J.* **467**, 819 (1996).
- [44] O. Sorlin, *et al.*, *Phys. Rev.* **C47**, 2941 (1993).
- [45] S. Starrfield, *et al.*, *Mon. Not. R. Astron. Soc.* **296**, 562 (1998).
- [46] R.E. Taam, *Ann. Rev. Nucl. Part. Sci.* **35**, 1 (1985).
- [47] R.E. Taam, S.E. Woosley, D.Q. Lamb, *Astrophys. J.* **459**, 271 (1996).
- [48] K. Takahashi, J. Witt, H.-T. Janka, *Astron. Astrophys.* **286**, 857 (1994).
- [49] J. Taylor, *Rev. Mod. Phys.* **66**, 711 (1994).
- [50] F.-K. Thielemann, M. Arnould, J.W. Truran, in *Advances in Nuclear Astrophysics*, ed. E. Vangioni-Flam, Gif sur Yvette, Editions Frontière, 1987, p.525
- [51] F.-K. Thielemann, *et al.*, *Nucl. Phys.* **A570**, 329c (1994).
- [52] F.-K. Thielemann, K. Nomoto, M. Hashimoto, *Astrophys. J.* **460**, 408 (1996).
- [53] F.-K. Thielemann, *et al.*, in *Nuclear and Particle Astrophysics*, eds. J. Hirsch, D. Page, Cambridge Univ. Press, 1998, p.27.
- [54] S.E. Thorsett, *Phys. Rev. Lett.* **77**, 1432 (1996).
- [55] E.P.J. van den Heuvel, D.R. Lorimer, *Mon. Not. R. Astron. Soc.* **283**, L37 (1996).
- [56] R.A. Wallace, S.E. Woosley, *Ap. J. Suppl.* **45**, 389 (1981).
- [57] G. Wallerstein, *et al.*, *Rev. Mod. Phys.* **69**, 995 (1997).
- [58] S.E. Woosley, *Ann. N.Y. Acad. Sci.* **759**, 446 (1995).
- [59] S.E. Woosley, W.D. Arnett, D.D. Clayton, *Ap. J. Suppl.* **26**, 231 (1973).
- [60] S.E. Woosley, *et al.*, *At. Data Nucl. Data Tables* **22**, 371 (1978).
- [61] S.E. Woosley, R.D. Hoffman, *Astrophys. J.* **395**, 202 (1992).
- [62] S.E. Woosley, *et al.*, *Astrophys. J.* **433**, 229 (1994).
- [63] C.T. Zhang, *et al.*, *Z. Phys.* **A358**, 9 (1997).